Effect of EUV light scattering from the rough absorber and buffer side

Yeong-keun Kwon, Jun-taek Park, Jong-hoi Kim, Byung-cheol Cha, Seung-wook Park
and Hye-keun Oh
Physics Department, Hanyang University, Korea

HANYANG UNIVERSITY

Contents

1. Introduction
2. Theory
3. Mathematical Description for the problem
4. Simulation results
5. Conclusions and Discussions

1. Introduction

- Light scattering for 13 nm wavelength are mostly attributed to the top surface roughness as well as the side wall roughness of the absorber and buffer or the etched wall of the mask for EUVL

- A bumpy side wall of an absorber and buffer that causes random scattering for the incident field, the scattered light will interfere with the light reflected from the reflective multilayer in the near field

- A random surface height variation (described by power spectral density) for the rough surfaces of EUVL is to be redefined to calculate the field in the image plane

- Multiple scattering on the three-dimensional rough surface should be derived and adopted for the dense pattern

2. Theory

Definition of Surface height variation

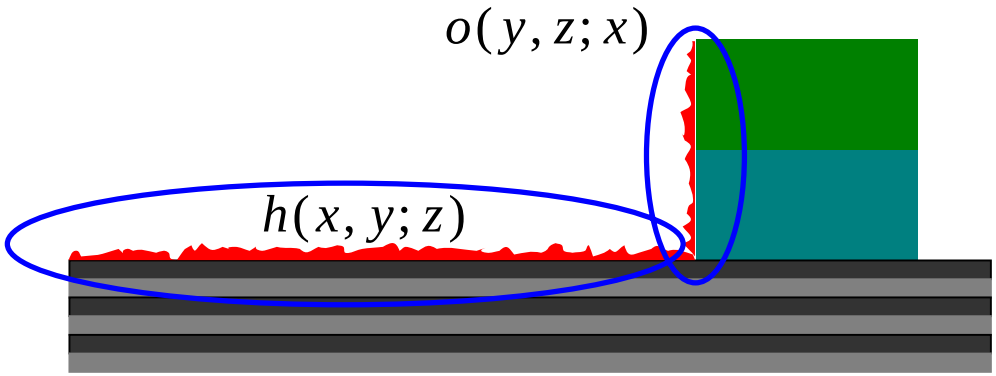

$$PSD(f,g)=\frac{1}{A}\left\langle\left|\int_A h(x,y)e^{-i2\pi(f\cdot x+g\cdot y)}dxdy\right|^2\right\rangle$$

$$PSD(g,m)=\frac{1}{A}\left\langle\left|\int_A o(y,z)e^{-i2\pi(g\cdot y+m\cdot z)}dydz\right|^2\right\rangle$$

Correlation problem for two independent height functions?

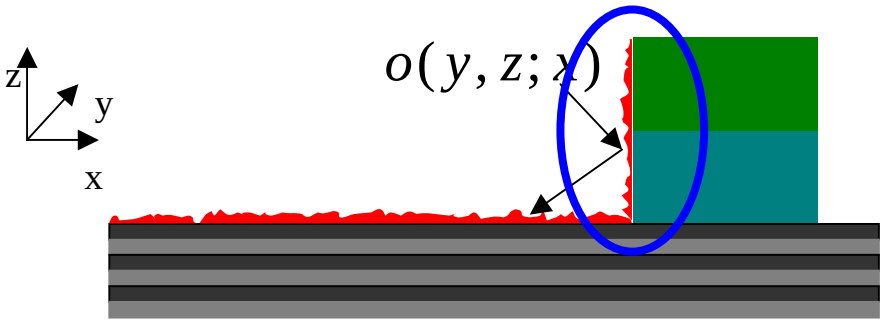

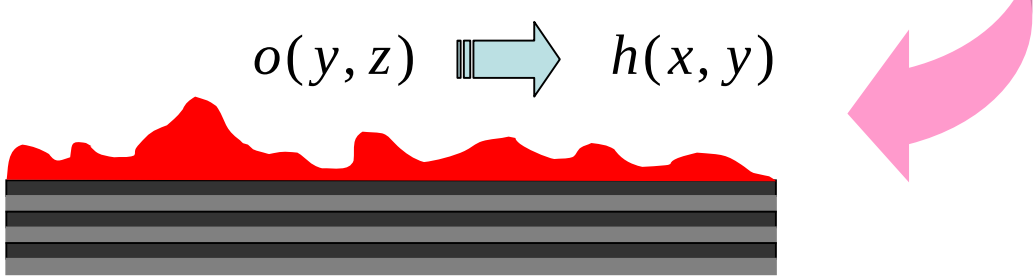

➢Height variation function for the side wall surface is treated the same manner of the rough x-y surface

Multiple scattering for dense pattern

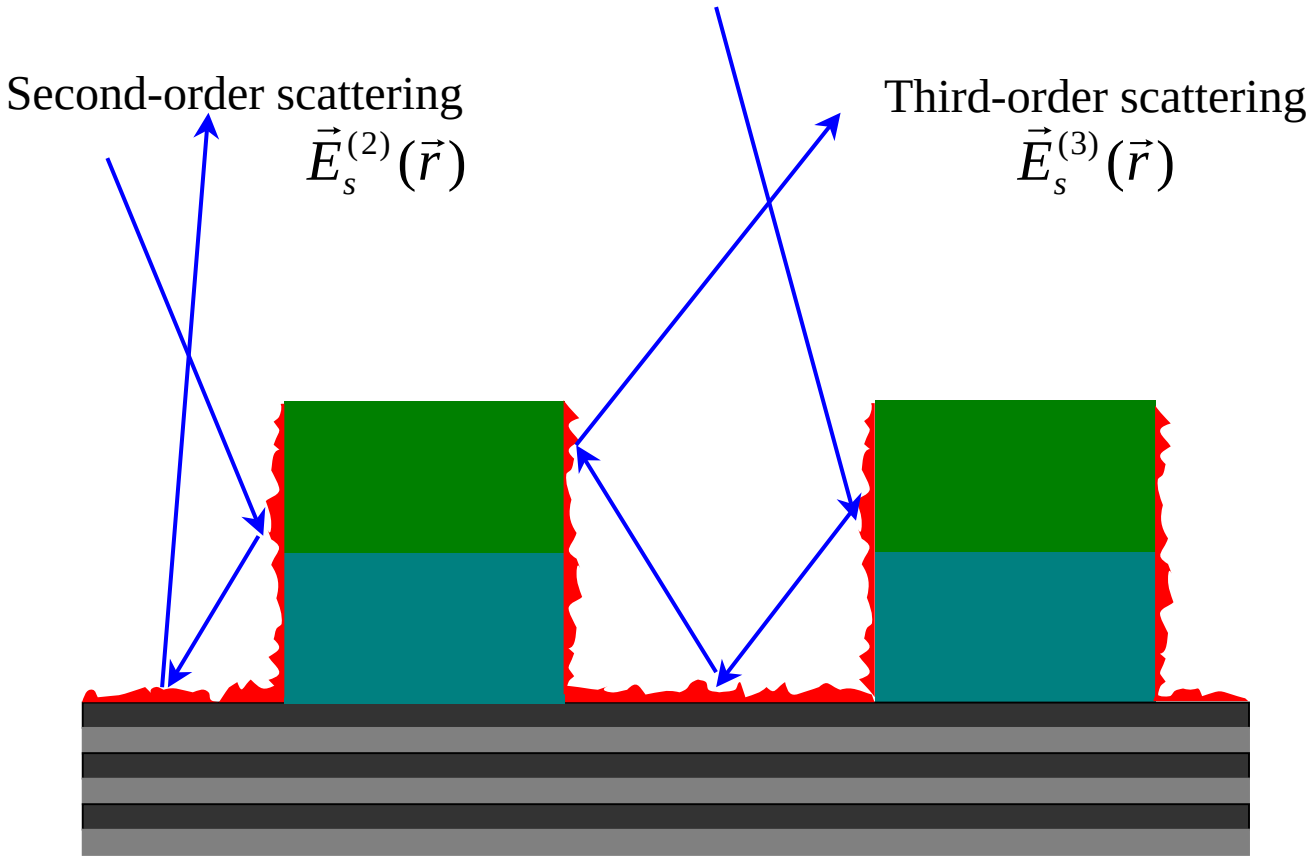

✓This is the mechanism by which energy is not transferred directly from the incident wave into the scattered wave may become ‘trapped’ within the well

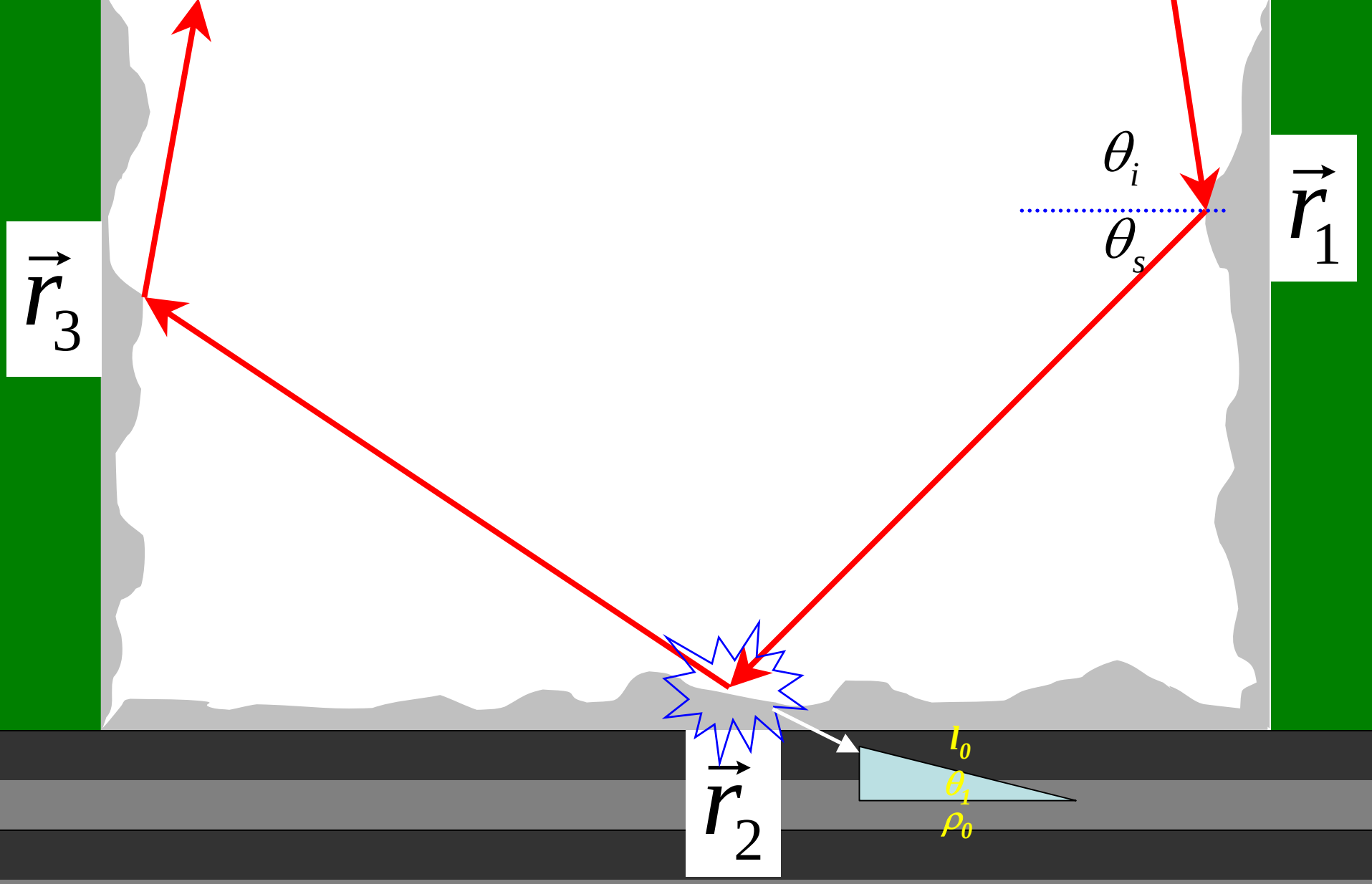

Figure 1.Geometry of the rough surface and scattering

3. Mathematical description for the problem

From Huygen's principle, the single scattered field from rough surface is

$$\vec{E}_s(\vec{r}) = \int_A d\vec{r}_{1\rho} \begin{bmatrix} i\omega\mu\bar{\bar{g}}(\vec{r},\vec{r}_1) & 0 \\ 0 & \nabla\times\bar{\bar{g}}(\vec{r},\vec{r}_1) \end{bmatrix} \cdot \begin{bmatrix} \hat{n}_1\times\vec{H}(\vec{r}_1) & 0 \\ 0 & \hat{n}_1\times\vec{E}(\vec{r}_1) \end{bmatrix}^T$$

$$\equiv \int_A d\vec{r}_{1\rho}\bar{\bar{G}}(\vec{r},\vec{r}_1)\cdot\bar{\bar{R}}(\hat{n}_1,\hat{k}_s,\hat{k}_i)\cdot\vec{E}_i(\vec{r}_1) \qquad (1)$$

$$\bar{\bar{g}}(\vec{r},\vec{r}_1) = \left(\bar{\bar{I}} + \frac{\nabla\nabla}{k^2}\right)\frac{\exp\left(ik\left|\vec{r}-\vec{r}_1\right|\right)}{4\pi\left|\vec{r}-\vec{r}_1\right|}$$

(2) : Dyadic Green's function in free space

$$\hat{n}_1 = \frac{-\partial_x\hat{x} - \partial_y\hat{y} + 1\hat{z}}{\sqrt{1+\partial_x^2+\partial_y^2}}$$

(3) : Normal vector at r_1

$$\partial_x = \frac{\partial h(x,y)}{\partial x}, \partial_y = \frac{\partial h(x,y)}{\partial y}$$

(4) Random height *h(x,y)* gradient

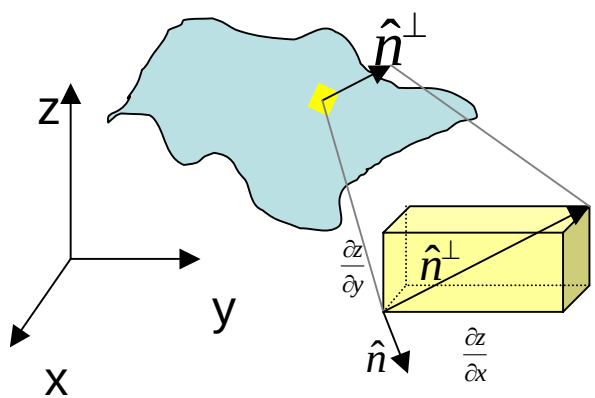

Figure 2.Geometry of the normal vector of the rough surface

$$\bar{\bar{G}}(\vec{r},\vec{r}_1) \equiv \begin{bmatrix} i\omega\mu\bar{\bar{g}}(\vec{r},\vec{r}_1) & 0 \\ 0 & \nabla\times\bar{\bar{g}}(\vec{r},\vec{r}_1) \end{bmatrix} \qquad (5)$$

$$\bar{\bar{R}}(\hat{n}_1,\hat{k}_s,\hat{k}_i)\cdot\vec{E}(\vec{r}_1) \equiv \begin{bmatrix} \hat{n}_1\times\vec{H}(\vec{r}_1) & 0 \\ 0 & \hat{n}_1\times\vec{E}(\vec{r}_1) \end{bmatrix}^T \qquad (6)$$

✓From the Kirchhoff approximation, the fields at any points on the surface are approximated by the fields present on the local tangent plane at that point

$$\overline{\overline{R}}\left(\hat{n}_1, \hat{k}_s, \hat{k}_i\right) \equiv \sqrt{1+\partial_x^2+\partial_y^2}\begin{bmatrix} -\left(\frac{1}{\eta}\right)\left(1-R_{//}\right)\left(\hat{n}_1\cdot\hat{k}_i\right)\hat{p}_{//}\hat{p}_{//} + \\ \left(\frac{1}{\eta}\right)\left(1+R_{\perp}\right)\left(\hat{n}_1\times\hat{p}_{//}\right)\hat{p}_{\perp} + \\ \left(1+R_{//}\right)\left(\hat{n}_1\times\hat{p}_{//}\right)\hat{p}_{//} + \\ \left(1-R_{\perp}\right)\left(\hat{n}_1\cdot\hat{k}_i\right)\hat{p}_{//}\hat{p}_{\perp} \end{bmatrix} \quad (7)$$

$R_{//}, R_{\perp}$

Local Fresnel reflection coefficients

$$\eta = \sqrt{\frac{\mu_0}{\varepsilon_0}}$$

$$\hat{p}_{//} = \frac{\hat{k}_i \times \hat{n}_1}{\left|\hat{k}_i \times \hat{n}_1\right|}, \quad \hat{p}_{\perp} = \hat{q}_i \times \hat{k}_i$$

(8) Initial local polarization vector around $\vec{r}_1$

✓In the far field approximation , eq.(9) , the dyadic Green's function becomes

$$k\left|\vec{r}-\vec{r}_1\right| = k\left(r^2 - 2\vec{r}_1\cdot r + r_1^2\right)^{1/2} \approx kr\left[1-\frac{\vec{r}_1\cdot r}{r^2}+O\left(\frac{r_1}{r}\right)^2\right] \approx kr - k\hat{r}\cdot\vec{r}_1 \quad (9)$$

$$\overline{\overline{g}}\left(\vec{r},\vec{r}_1\right) = \left[\frac{\exp(ikr)}{4\pi r}\right]\left(\hat{p}_{s//}\hat{p}_{s//} + \hat{p}_{s\perp}\hat{p}_{s\perp}\right)\exp\left(-i\vec{k}_s\cdot\vec{r}_1\right) \quad (10)$$

Polarization vector after scattering

$$\hat{p}_{s//} = \frac{\hat{k}_s \times \hat{z}}{\left|\hat{k}_s \times \hat{z}\right|}, \quad \hat{p}_{s\perp} = \hat{p}_{s//} \times \hat{k}_s \tag{11}$$

$$\left(\bar{\bar{I}} + \frac{\nabla\nabla}{k^2}\right)\vec{E} = \begin{bmatrix} \hat{p}_{s//}\hat{p}_{s//} & 0 \\ 0 & \hat{p}_{s\perp}\hat{p}_{s\perp} \end{bmatrix}\vec{E} \tag{12}$$

Diagonalization of the eigen value in equation (10)

✓In the high-frequency limit, the scattered power is principally contributed by the specular stationary phase points. At the stationary point, the normal vector is

$$\hat{n}_{10} = -\frac{\delta\vec{k}_0}{\left|\delta\vec{k}_0\right|} = \frac{-\partial_{0x}\hat{x} - \partial_{0y}\hat{y} + \hat{z}}{\sqrt{1 + \partial_{0x}^2 + \partial_{0y}^2}} \tag{13}$$

Here,

$$\delta\vec{k}_0 \equiv \hat{k}_i - \hat{k}_s, \quad \partial_{0x} = -\frac{\delta k_{0x}}{\delta k_{0z}}, \quad \partial_{0y} = -\frac{\delta k_{0y}}{\delta k_{0z}} \tag{14}$$

First-order (single) scattered field

$$\vec{E}_s^{(1)}(\vec{r}) = \int_A d\vec{r}_{1\rho} \overline{\overline{G}}(\vec{r},\vec{r}_1)\cdot \overline{\overline{R}}(\hat{n}_1,\hat{k}_s,\hat{k}_i)\cdot \vec{E}_i^{\,0}(\vec{r}_1)$$

$$= \left[\frac{ik\exp(ikr)}{4\pi r}\right](\hat{p}_{s//}\hat{p}_{s//} + \hat{p}_{s\perp}\hat{p}_{s\perp})\cdot \overline{\overline{R}}_0(\hat{k}_s,\hat{k}_i)\cdot \hat{e}_i E_0 \int_A d\vec{r}_{1\rho}\, \exp\left[i(\vec{k}_i - \vec{k}_s)\cdot \vec{r}_1\right] \tag{15}$$

Where,

$$\overline{\overline{R}}_0(\hat{k}_s,\hat{k}_i) = \sqrt{1+\partial_{0x}^2+\partial_{0y}^2}\left\{\begin{array}{l} -(1-R_{//})(\hat{n}_{10}\cdot\hat{k}_i)\hat{p}_{//}\hat{p}_{//} + \\ (1+R_{\perp})(\hat{n}_{10}\times\hat{p}_{//})\hat{p}_{\perp} + \\ (1+R_{//})\left[\hat{k}_s\times(\hat{n}_{10}\times\hat{p}_{//})\right]\hat{p}_{//} + \\ (1-R_{\perp})(\hat{n}_{10}\cdot\hat{k}_i)(\hat{k}_s\times\hat{p}_{//})\hat{p}_{\perp} \end{array}\right\}, \tag{16}$$

$$\vec{E}_i^{\,0}(\vec{r}_1) = \hat{e}_i E_0 \exp(i\vec{k}_i\cdot\vec{r}_1), \qquad \hat{e}_i = \hat{p}_{s//}\ or\ \hat{p}_{s\perp} \tag{17}$$

Second-order scattered field

$$\vec{E}_s^{(2)}(\vec{r}) = \int_A d\vec{r}_{2\rho} \int_A d\vec{r}_{1\rho} \overline{\overline{G}}(\vec{r},\vec{r}_2)\cdot\overline{\overline{R}}(\hat{n}_2,\hat{k}_s,\hat{k}_1)\overline{\overline{G}}(\vec{r}_2,\vec{r}_1)\cdot\overline{\overline{R}}(\hat{n}_1,\hat{k}_1,\hat{k}_i)\cdot\vec{E}_i^{\,0}(\vec{r}_1) \quad (18)$$

$$\vec{E}_s^{(2)}(\vec{r}) = \left[\frac{ik\exp(ikr)}{4\pi r}\right]\left\{\begin{array}{l}\int_A d\vec{r}_{2\rho}\int_A d\vec{r}_{1\rho}\ \exp\left[i\delta\vec{k}_2\cdot\vec{r}_2\right]\exp\left[i\delta\vec{k}_1\cdot\vec{r}_1\right]\left(\hat{p}_{s//}\hat{p}_{s//}+\hat{p}_{s\perp}\hat{p}_{s\perp}\right)\\ \cdot\overline{\overline{R}}_0(\hat{k}_s,\hat{k}_1)\dfrac{ik}{4\pi\tau_0}\cdot\left(\hat{p}_{s//}\hat{p}_{s//}+\hat{p}_{s\perp}\hat{p}_{s\perp}\right)\cdot\overline{\overline{R}}_0(\hat{k}_1,\hat{k}_i)\cdot\hat{e}_i E_0\end{array}\right\} \quad (19)$$

The far-field approximation for $\overline{\overline{g}}(\vec{r},\vec{r}_2)$ and the dyadic Green's function

$$\overline{\overline{g}}(\vec{r}_2,\vec{r}_1) \approx \left[\frac{1}{4\pi l_0}\right]\left(\hat{p}_{s//}\hat{p}_{s//}+\hat{p}_{s\perp}\hat{p}_{s\perp}\right)\exp\left(-i\vec{k}_1\cdot(\vec{r}_2-\vec{r}_1)\right) \quad (20)$$

$$l_0 = |\vec{r}_2-\vec{r}_1|, \quad \delta\vec{k}_1 \equiv \vec{k}_i-\vec{k}_1, \delta\vec{k}_2 \equiv \vec{k}_1-\vec{k}_s, \quad (21)$$

$$\hat{n}_{10} = \frac{|\delta k_{1z}|\delta\vec{k}_1}{\delta k_1|\delta\vec{k}_1|}, \hat{n}_{20} = \frac{|\delta k_{2z}|\delta\vec{k}_2}{\delta k_{2z}|\delta\vec{k}_2|} \quad (22)$$

normal vectors at $\vec{r}_1, \vec{r}_2$

At a fixed normal vector, the rebounced ray $\vec{k}_1$ is determined by $\hat{n}_{10}$ then $\hat{n}_{20}$ is determined afterwards

$$\vec{r}_2 = \vec{r}_1 + l_0\hat{k}_1, \quad \vec{r}_{1\rho} = r_1 \sin\theta_i \left(\cos\phi_0 \hat{x} + \sin\phi_0 \hat{y}\right)$$

$$l_0 = \frac{\rho_0}{\cos\theta_1}$$

$$\vec{r}_{2\rho} = \vec{r}_{1\rho} + \rho_0 \left(\cos\phi_1 \hat{x} + \sin\phi_1 \hat{y}\right) \quad (23)$$

$$\int_A d\vec{r}_{1\rho} \int_A d\vec{r}_{2\rho} = \int_A d\vec{r}_{1\rho} \int_0^{\infty} \rho_0 d\rho_0 \int_0^{2\pi} d\phi_1$$

(24) : Solid Angle transformation in eq. (18)

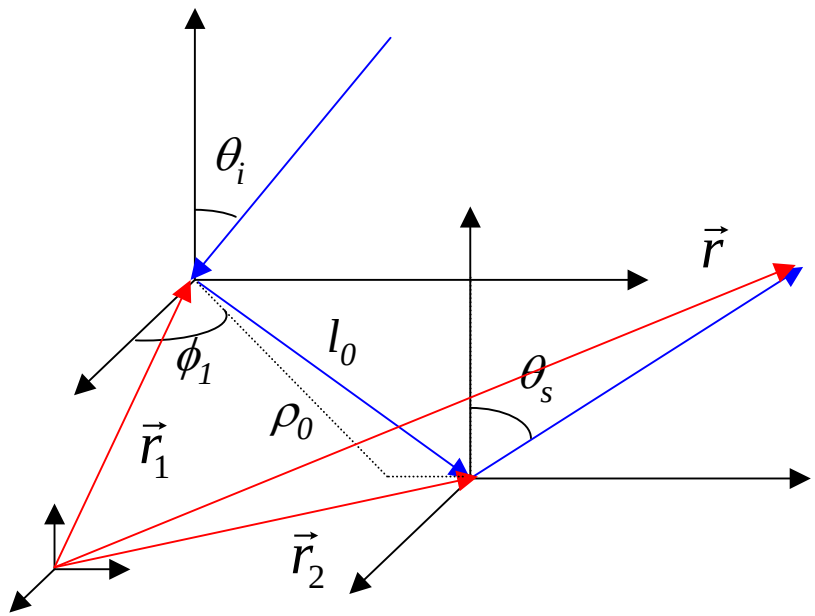

Figure 3. Polar coordinate scheme

The general formula of n-th scattered electric field and its dyadic Green's function

$$\vec{E}^{n}(\vec{r}_n) = \int_A dr_{n-1}\,\overline{\overline{G}}(\vec{r}_n,\vec{r}_{n-1})\cdot\overline{\overline{R}}(\hat{n}_n,\vec{k}_n,\vec{k}_{n-1})\cdot\overline{\overline{G}}(\vec{r}_{n-1},\vec{r}_{n-2})\cdot\overline{\overline{R}}(\hat{n}_{n-1},\vec{k}_{n-1},\vec{k}_{n-2})E^{n-2}(\vec{r}_{n-2})$$

$$= \int_A dr_{n-1}\int_A dr_{n-2}\cdots\int_A dr_1\,\overline{\overline{G}}(\vec{r}_n,\vec{r}_{n-1})\cdot\overline{\overline{R}}(\hat{n}_n,\vec{k}_n,\vec{k}_{n-1})\cdots\overline{\overline{G}}(\vec{r}_2,\vec{r}_1)\cdot\overline{\overline{R}}(\hat{n}_2,\vec{k}_2,\vec{k}_1)E^{1}(\vec{r}_1)$$

$$= \prod_{m=1}^{n-1}\left[\int_A dr_m\,\overline{\overline{G}}(\vec{r}_{m+1},\vec{r}_m)\cdot\overline{\overline{R}}(\hat{n}_m,\vec{k}_m,\vec{k}_{m-1})\right]E(\vec{r}) \qquad (25)$$

$$\overline{\overline{g}}(\vec{r}_{m+1},\vec{r}_m) \approx \frac{e^{ik|\vec{r}_{m+1}-\vec{r}_m|}}{4\pi|\vec{r}_{m+1}-\vec{r}_m|}\left(\hat{p}_{m+1s//}\hat{p}_{m+1s//} + \hat{p}_{m+1s\perp}\hat{p}_{m+1s\perp}\right)e^{-i\vec{k}_m\cdot(\vec{r}_{m+1}-\vec{r}_m)} \qquad (26)$$

The multiple scattering field taken all of high-order scatterings in written as

$$\vec{E}_s(\vec{r}) = \sum_{n=1}^{\infty}\vec{E}_s^{(n)}(\vec{r}) \qquad (27)$$

4. Simulation result

Incidence angle	Wavelength	Absorber & buffer height	Absorber & buffer	Pattern type
6°	13.5 nm	150 nm	Cr and SiO_2	30 nm isolate line

Near-field phase variation on x-z plane

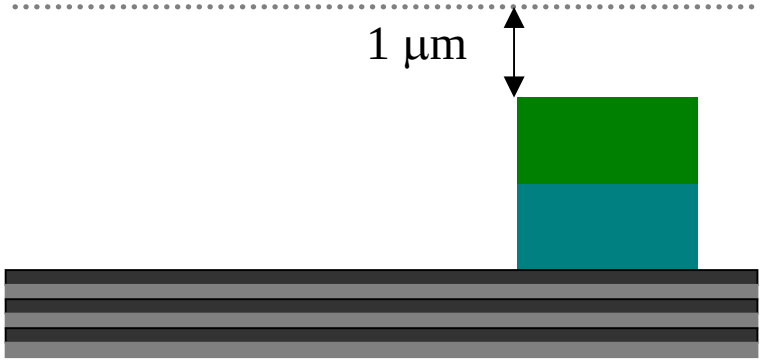

(a) Flat surface

(b) Rough surface

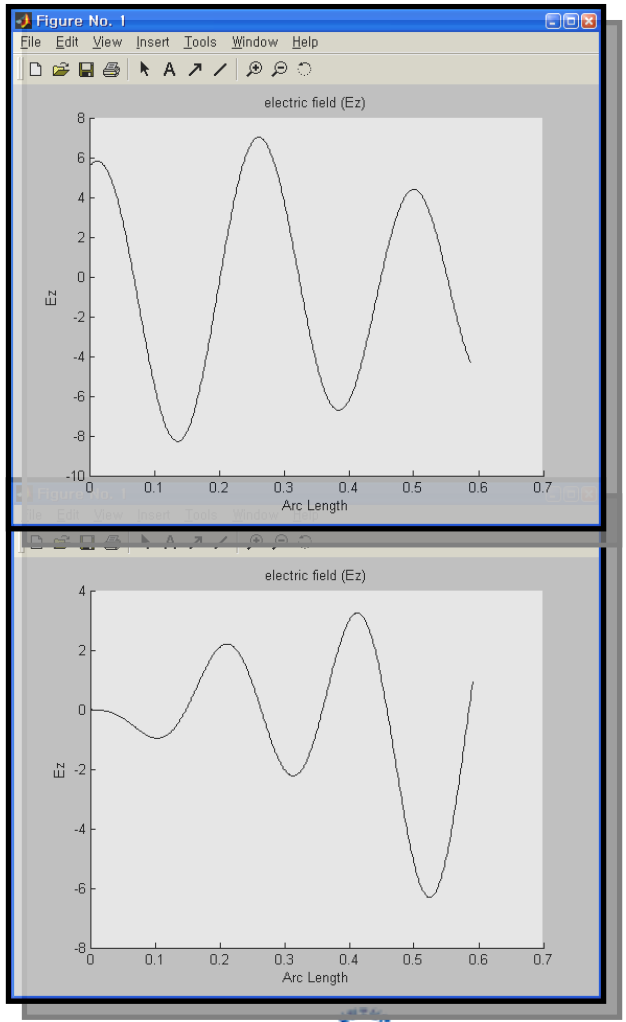

Figure 4. Second-order scattering scheme and results

Incidence angle	Wavelength	Absorber & buffer height	Absorber & buffer	Pattern type
6°	13.5 nm	150 nm	Cr and SiO_2	1:1 30 nm dense line & space

Near-field phase variation on x-z plane

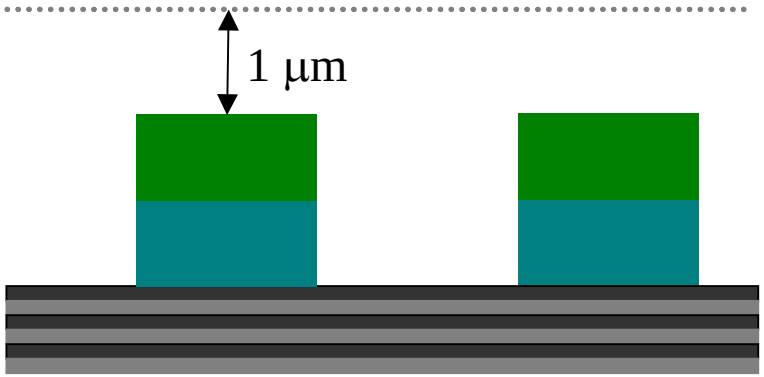

(a) Flat surface

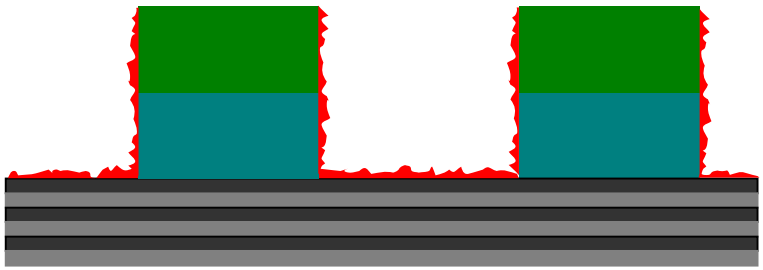

(b) Rough surface

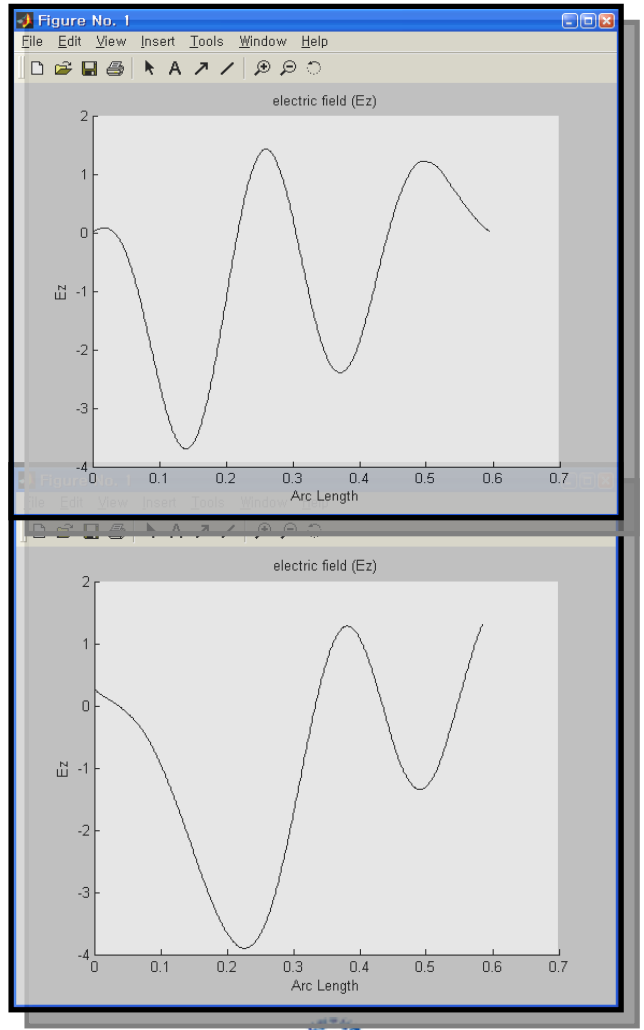

Figure 5. Third-order scattering scheme and results

4. Conclusions and Discussions

1. Scattering, not only on the rough multi-layer's surface but also on the rough absorber and buffer side wall, should be considered to clarify E-field phase variation in the far field
2. From the Huygen's principle, scattered field is explicitly derived by using the dyadic Green's function for generality with appropriate approximations
   - Height function, *O(y,z)*, of the rough side wall, causing multiple scattering, is converted into x-y plane rough surface
   - Kirchhoff theory is effective for approximating the field on the rough surface
   - Observation is in the far field of the surface
   - The incident wave is planar and monochromatic
   - No point on the rough surface has infinite gradient
3. A general formula for the n-th scattered electric field is analogous to Feynmann's approach to scattering
4. There are significant near-field variations in phase and amplitude for the rough surface compared to the flat mirror structure in
5. Unfortunately, more detailed simulation results from various points of view are not available at the moment, it is expected in the near future